[Frontiers in Bioscience 19, 1227-1239, June 1, 2014]

Lung tissue engineering

David M. Hoganson[1,2], Erik K. Bassett[1], Joseph P. Vacanti[1]

[1]Center for Regenerative Medicine, Department of Surgery, Massachusetts General Hospital, Boston, MA USA, [2]Department of Surgery, Washington University in St. Louis, St. Louis, MO USA

TABLE OF CONTENTS

1. ABSTRACT

Lung tissue engineering is an emerging field focused on the development of lung replacement devices and tissue to treat patients with end stage lung disease. Microfluidic based lung assist devices have been developed that have biomimetically designed vascular networks that achieve physiologic blood flow. Gas exchange in these devices occurs across a thin respiratory membrane. Designed for intrathoracic implantation as a bridge to transplant or destination therapy, these lung assist devices will allow ambulation and hospital discharge for patients with end stage lung disease. Decellularized lungs subsequently recellularized with epithelial and endothelial cells have been implanted in small animal models with demonstration of initial gas exchange. Further development of these tissues and scaling to large animal models will validate this approach and may be an organ source for lung transplantation. Initial clinical success has been achieved with decellularized tracheal implants using autologous stem cells. Development of microfluidic lung models using similar architecture to the lung assist device technology allows study of lung biology and diseases with manipulation of lung cells and respiratory membrane strain.

2. INTRODUCTION

Tissue engineering as a field aims to develop clinical therapies that recreate or promote a natural recapitulation of human organs and soft tissues. Early experiences, before the field of tissue engineering was well defined, focused on skin replacements (1-3). The primary clinical successes to date have been limited to soft tissues including cellularized biologic dressings (4). Engineered small diameter blood vessels (5, 6), bladder (7) and cellular therapy for damaged myocardium (8) are currently being evaluated in clinical trials.

Lung replacement technology, in the forms of cardiopulmonary bypass and extracorporeal membrane oxygenation, are now routine clinical therapies but their use is restricted to the operating room or an intensive care unit. Much work has been done to transition this technology to an implantable lung assist device, but this is still a work in progress. Recently a pumpless hollow fiber lung assist device has been approved for acute lung injury and has been used in an intensive care setting (9-11).

Compared to mechanical lung replacement technology, cellular based lung tissue engineering is still a

very nascent field with significant progress being achieved in the last five years. The native lung has a phenomenal surface area to volume ratio achieving 70 to 100 m^2 of gas exchange surface with a branching airway network ending in 200 micron diameter alveolar sacs. These sacs intersect a branching vascular network that divides 5 L/min of blood flow into pulmonary capillaries separated from the alveoli by the thin respiratory membrane. Among the most remarkable of human tissues, the human respiratory membrane averages just 0.5 microns in thickness which allows the efficient exchange of oxygen and carbon dioxide.

The complex three dimensional anatomical structure of the lung has made reproduction of this tissue challenging. Scaffolding approaches are now being developed to integrate the vascular and airway structures to achieve gas exchange. Engineered scaffolds that are under development utilize porous polymers or microfluidic networks to create the vascular and airspace structures of the lung (12-14). Decellularized lung scaffolds are a second scaffold approach that utilizes the native extracellular matrix structure as the scaffold (15, 16). As with all engineered tissues, selecting and managing cells for populating the scaffolds are a challenge independent of the scaffold development method. The goal is to utilize autologous (primary or stem) cells to seed the vascular and pulmonary components of the engineered lung. In just the last few years, the stem cell community has made significant strides to this end.

Although an implantable tissue engineered lung is certainly several years in the future, tissue engineering principles are being applied to development of *in vitro* models of lung tissue (17). These models have the dual purpose to further our understanding of lung biology and mechanics to accelerate engineered tissue development and serve as models of lung disease to screen and test important lung drugs and other therapies.

3. ENGINEERED SCAFFOLD APPROACH

The challenge of scaffold development for the lung is centered on the creation of two independent 3D systems: the branched vascular network and the airspace. These systems lead to capillary and alveoli analogs where gas exchange can occur. The vascular and airspace networks need to be separated by a gas permeable membrane with a large surface area that can efficiently allow diffusion of oxygen and carbon dioxide.

3.1. Vascularized scaffold architecture

Early solid organ tissue engineering efforts were limited by obtaining adequate cell thickness without central necrosis. Diffusion of oxygen and nutrients from a blood vessel is limited to only a few hundred microns but in highly metabolic tissues, that functional distance is even less. This requires a blood vessel network for a solid organ to be an expansive 3D structure. Angiogenesis has been investigated as a means of creating blood vessels for tissue engineering applications (18-20). Angiogenesis is limited as an architectural approach because it cannot address the need for creation of the larger vessels to connect to the spontaneous capillary network. A tissue engineered lung will need to immediately handle all of the cardiac output when surgically implanted, therefore the large artery and vein vessels need to be fully developed and connected to the capillary like exchange vessels of the scaffold for immediate use. Additionally, the capillary like vessels of the lung scaffold will need to be intimately related to the alveoli structures and there is no evidence that a spontaneous angiogenesis network can efficiently achieve this.

A vascularized scaffold architecture has been developed as an approach for creation of a tissue engineered lung (14). This architecture is based on the vascularized liver tissue engineering scaffolds (21, 22) developed by the Vacanti group to overcome the limitations of angiogenesis in liver tissue engineering. The central architectural concept of the engineered lung scaffold is a network of branching blood vessels created from the pulmonary artery down to lung capillary like vessels and then recollect into pulmonary veins. Analogous to the liver scaffold where the blood vessel network is positioned adjacent to hepatocytes, in the lung scaffold, the vascular network is positioned adjacent to an alveolar chamber. Blood flows through the microfluidic vascular network and oxygen flows through the adjacent alveolar chamber. Oxygen and carbon dioxide are exchanged across a respiratory membrane that separates the two.

The first generation lung technology utilized a branching vascular network 200 microns in depth (Figure 1). Three gas exchange membranes were tested; 64 microns thick silicone gas exchange membrane, porous membrane and porous membrane with 3 microns silicone coating. *In vitro* gas exchange testing demonstrated increasing exchange of oxygen and carbon dioxide with increasing flow rates with all three membranes (Figure 2). There was no significant difference between the membranes, but these were first generation membranes for a planar lung scaffold technology. This initial scaffold demonstrated the potential utility of this lung architecture as a step toward development of a tissue engineered lung.

Although the first generation vascularized lung scaffold demonstrated efficient gas exchange, the vascular network was mono depth with non-physiologic blood flow in portions of the vascular network. The vascular network design approach was then readdressed to create a vascular network design with physiologic blood flow. A series of design principles, based on biomimetic vessel dimensions and properties, were developed to achieve physiologic blood flow first in a tissue engineered liver scaffold (23). These design principles were applied to the vascularized lung architecture and a second generation vascularized lung scaffold was developed (24) (Figure 3).

Physiologic blood flow is a centrally important aspect of a tissue engineered lung scaffold. Shear stress is maintained within a narrow range in native blood vessels to avoid activation of platelets that would trigger platelet adhesion and thrombus formation. Physiologic shear stress

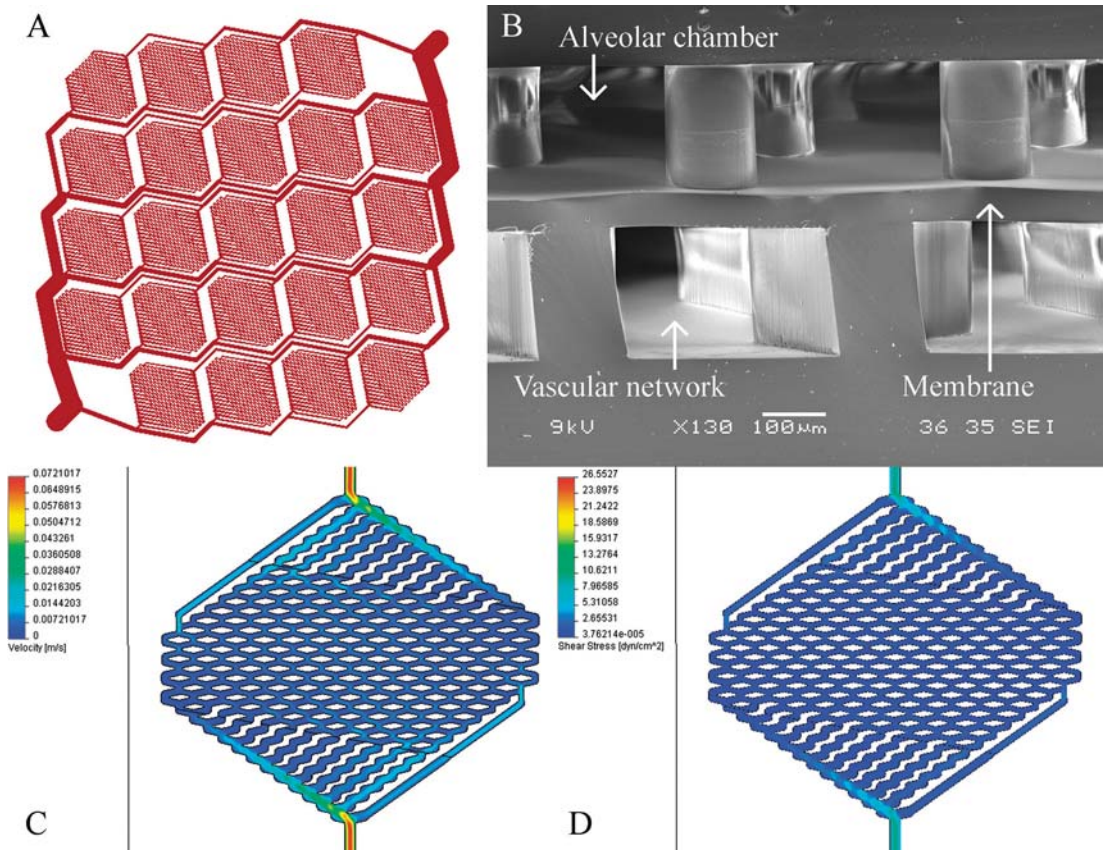

Figure 1. Design of vascular network based lung assist device. A, Top view of branched vascular network design with single blood inlet and single blood outlet. B, Cross-sectional SEM image of cut edge of device with silicone membrane. C and D: Velocity plot C) and D) shear stress plot from CFD analysis of capillary like area of vascular network at blood flow rate of 4 ml/min. Reproduced with permission from (14).

must be achieved within the scaffold to minimize platelet activation and thrombosis. Additionally, once a complete endothelial lining of a tissue engineered scaffold has occurred, as long as the design achieves physiologic shear stress, anticoagulation should be able to be withdrawn.

The second generation vascular scaffold has shear stresses (14 - 56 dynes/cm^2) in the range of normal arterial shear stress (10 - 70 dynes/cm^2) (25). Computational fluid dynamics (CFD) analysis was used during the vascular network design process to iteratively analyze the flow characteristics within the device after each design change. Many aspects of the design were optimized with the CFD data to achieve a high density network with minimal shear stress changes at the bifurcations and trifurcations. To achieve physiologic shear stress, an important shift in design and manufacturing was made to create 3D networks with variable depths. For previous vascular networks and within the field of microfluidics in general, photolithography is used as the manufacturing process to create the molds. Photolithography is limited to a single depth or a few discrete depths with no design control over the depth interfaces. Micro milling is an emerging technology that was used to create a 3D mold with each of the channels having a depth equal to the channel width (Figure 3). This manufacturing technology has accuracy to 2 microns and allows precise dimensions including complex bifurcation fillets to achieve optimal flow conditions. The resistance of the network to flow was determined prospectively so after implantation the scaffold would have the desired blood flow. *In vitro* testing of the network with blood demonstrated excellent correlation with the CFD predicted flows. Gas exchange within the network was comparable to current hollow fiber oxygenators per unit of surface area utilizing an improved silicone gas exchange membrane 8.7 ± 1.2 microns thick.

Other groups have also developed microfluidic based gas exchange devices. Burgess et.al. reported development of a microfluidic based lung device with vascular channels 100 microns wide and 33 microns deep (13). The straight vascular channels of this first generation device are separated from gas layers by membranes as thin as 64 microns. These devices were tested for gas permeance rather than blood based gas transfer. The devices with 64 microns membranes had max permeance for oxygen and carbon dioxide of 9.16 x 10^{-6} and 3.55 x 10^{-5} ml/sec/cm^2/cmHg . These silicone based devices were also seeded with endothelial cells (EC) following coating with fibrinogen and the ECs were grown to confluence.

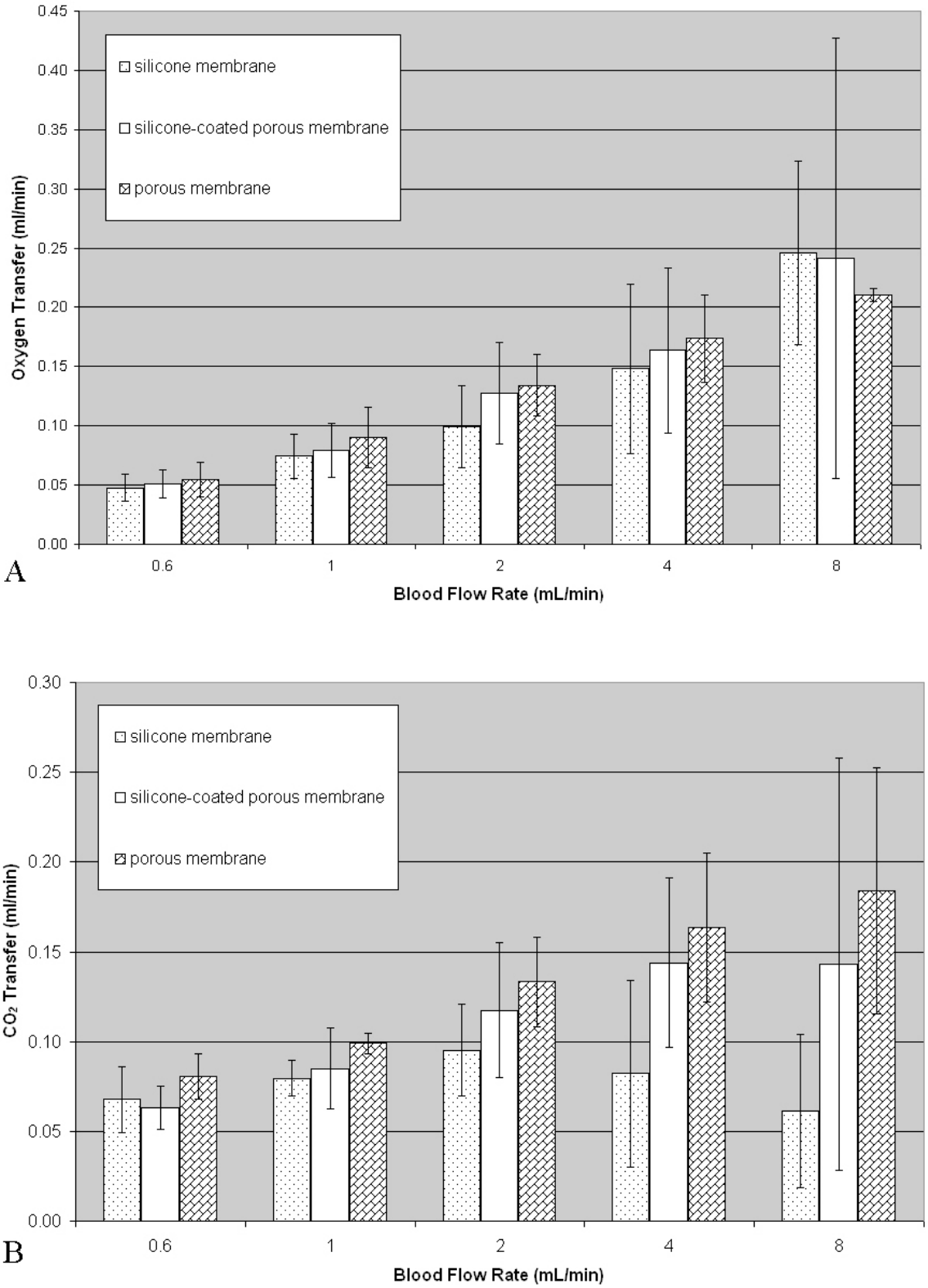

Figure 2. A) Oxygen transfer in lung assist device over range of blood flow rates. B) Carbon dioxide transfer in lung assist device over range of blood flow rates. Reproduced with permission from (14).

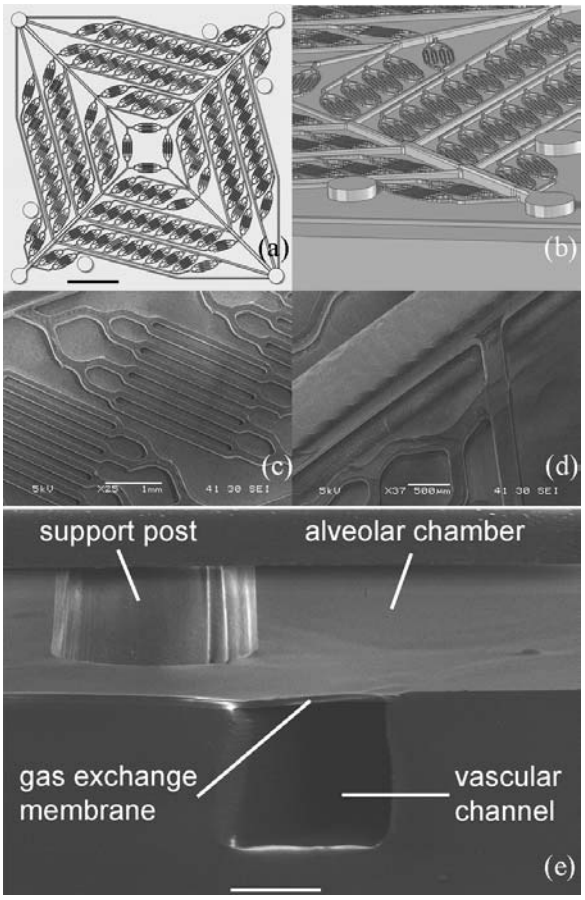

Figure 3. Design of lung vascular network with physiologic blood flow. (a) Top view of high density vascular network design, (b) isometric view of SolidWorks rendering of mold demonstrating variable depths and 1:1 aspect ratios of all channels, (c) SEM of smallest channels of device, (d) SEM of transition between large inlet channel and branch channel demonstrating precise 3D fillets achieved with micro machined mold. Scale bar in (a, c, d) = 1 cm. (e) Isometric cross-sectional view SEM of the device showing the three components of the device; alveolar chamber, gas exchange membrane and vascular network. Scale bar (e) = 100 microns. Reproduced with permission from (24).

These authors also note the significant potential benefit of a lung assist device with a confluent endothelial cell layer as anticoagulation may be reduced or avoided all together.

There as been some significant theoretical work in the area of predicting gas exchange in microfluidic channels (26-28) and comparing potential geometries of microfluidic lung devices for efficiency of gas transfer (12). Round and rectangular channels have been compared with varying diameters and channel lengths to calculate predicted total number of channels for a theoretical lung assist device (12). There is a balance as the predictions favor fewer required channels for geometries that do not have a 1:1 width to depth aspect ratio. The fewest channels are required in the geometries with screen filled channels with 40 microns depths and 15 mm widths but from a hemodynamic standpoint this has significant implications for non-ideal shear stress distributions and would not likely be a sustainable geometry from a clotting perspective. In contrast, the 25 microns circular channels required significantly more channels but could be constructed with hemodynamic profiles for physiologic shear stress likely capable of sustaining flow with anticoagulated blood. A microchannel concept device using a screen filled channel to create 40 microns to 82 microns channels was built and tested for oxygen exchange (29). This device gas exchange data confirmed the general principles of gas exchange balance observed in these devices including that the smaller depth channels have much higher increase in pO_2 and oxygen saturation than the deeper channels, given the same residence time. As the residence time increases, the oxygen saturation percent increases with a steeper increase for the 40 microns channels than the 82 microns channels. The overall oxygen exchange was similar for the 40 microns and 82 microns devices. These devices were constructed with 100 microns thick silicone membranes as the gas exchange membrane and there was little change in the oxygen exchange when a 200 microns silicone membrane was used. The screen filled channels induced a significant amount of blood mixing which certainly changed the relative resistance of the limitation of oxygen diffusion through the plasma fraction to RBCs distant from the gas exchange membrane and may have also changed the relative impact of changes in membrane gas permeability. In fact, this device achieved better oxygen transfer than would be predicted by the limitation of the plasma fraction to oxygen transfer through the depth of the channel, signifying that significant mixing is occurring. Although this design is an important step in furthering our understanding of gas exchange parameters these devices, the non-physiologic shear stress and flows that are likely present in this device may limit the clinical application secondary to induced clotting at clinically acceptable levels of anticoagulation.

Similar to the device developed by Burgess, another straight channel lung device was developed to investigate the fundamental gas exchange (30). A microfluidic device with straight channels 300 microns wide by 15 microns deep was compared to a device with channels consisting of 300 microns wide spaces between 200 microns diameter support posts in a 3 mm wide channel. Fundamentally, the differences in oxygen transfer and change in percent saturation between the devices was investigated. Similar to the data presented by Kung (29), there was in increase in the oxygen transfer or oxygen flux with a decrease in residence time. That is, the higher the blood flow rate through the device, the higher the oxygen transfer. This is also consistent with the data from the Hoganson *et al* devices and the body of hollow fiber based gas transfer devices. Also similar to the Kung data, in these 15 microns deep channels, there is a consistent increase in oxygen saturation with increased residence time of the blood in the channels. Likewise, the more shallow 15 microns channels achieved higher increase in oxygen

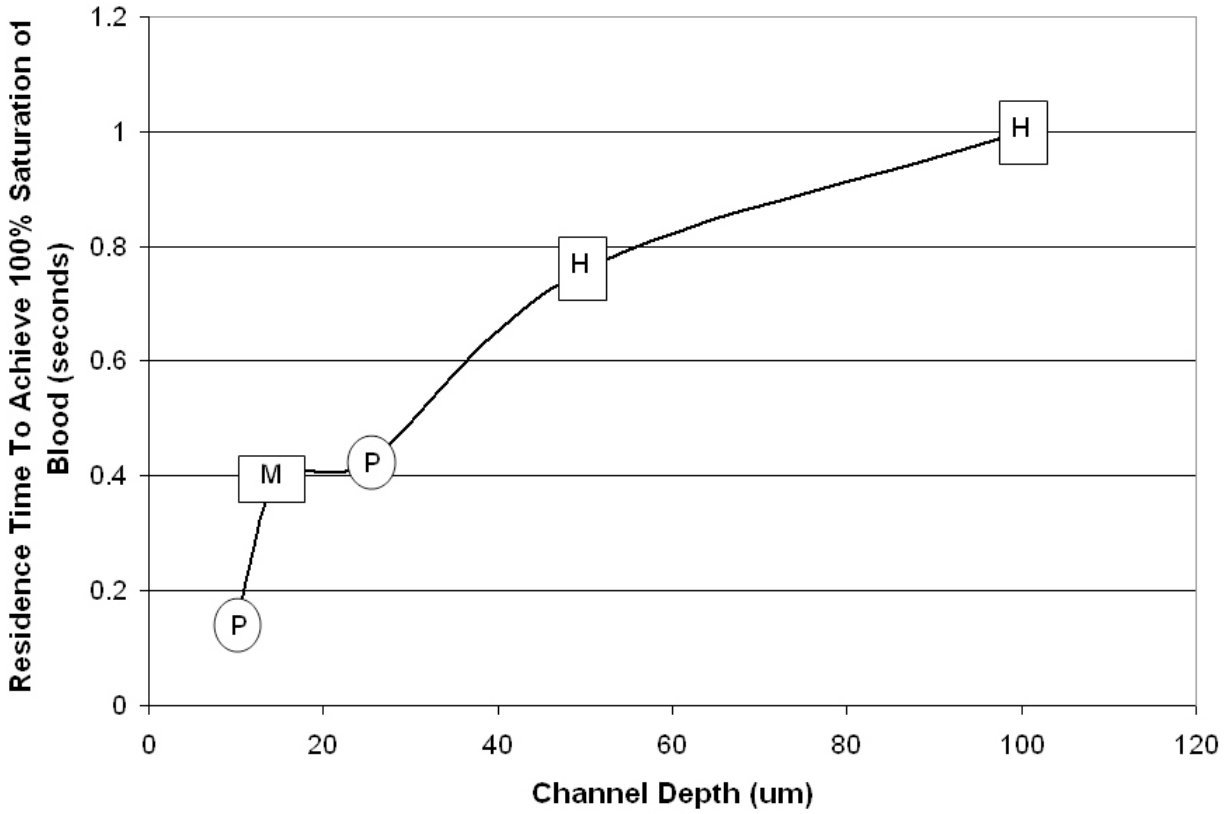

Figure 4. Residence time in lung device capillary channel required to achieve complete saturation of blood compared to the depth of the vascular channel. With increasing channel depth, the residence time required for the blood to become completely saturated is increased.

saturation with shorter residence times than the 40 or 82 microns channels. These data are consistent with previous experimental data by Page *et al* in 10 and 25 microns diameter channels that showed again an increase in oxygen saturation with longer residence time. In those dataset, the time to 100% oxygen saturation in the 10 microns channel was 0.2 sec while the time to full saturation in the 25 microns channel was 0.8 sec, a 4 fold difference. Considering the available data on oxygen saturation relative to channel depth and residence time, Figure 4 was constructed using data from Page *et al*, Kung (with some interpolation) and our own unpublished data. This graph demonstrates the clear relationship between channel depth and increasing required residency times to achieve complete blood saturation.

These geometrically simple devices serve to both highlight the potential of microfluidic gas exchange devices to function as lung assist devices and start to elucidate the design tradeoffs and particular design points that are critical to achieve adequate gas exchange. Regarding oxygen, there is are three clear variables that impact oxygen saturation in these devices; residence time of the red blood cell exposed to the gas exchange membrane or fundamentally blood velocity for a fixed exposure length, channel depth and blood mixing. We believe that laminar flow and physiologic shear stress are of central importance to minimize blood clot formation in these devices so no mixing strategies should be considered for an implantable or even medium length extracorporeal support device. Therefore the two design variables to be considered are channel depth and residence time. Ideally channel depths of 10 microns or less could be used similar to the native lung but that would almost assuredly result in uniform thrombosis without endothelialized channels. Even with physiologic shear stresses through the vascular network of a device and optimized flow, there is still a likely minimum channel size that can support flow without clot formation with clinically acceptable levels of anticoagulation. Hollow fiber devices with their 200 – 300 microns spacing between fibers suggest that a similar size range in a hemodynamically optimized device would be acceptable. Without *in vivo* testing, the minimum channel size will not be known. Our expectation is that it is in the range of 50 – 100 microns but that is purely speculative. The residence time or exposure time is a balance of velocity and length of gas exchange membrane. This balance should be adjusted for these devices so 100% saturation of the blood is attained but further increases in the pO_2 beyond that level is likely of very little benefit and costly in terms of design balance (longer channels, larger device, etc.).

Not all authors have investigated CO_2 gas exchange but in our devices, the CO_2 exchange with the

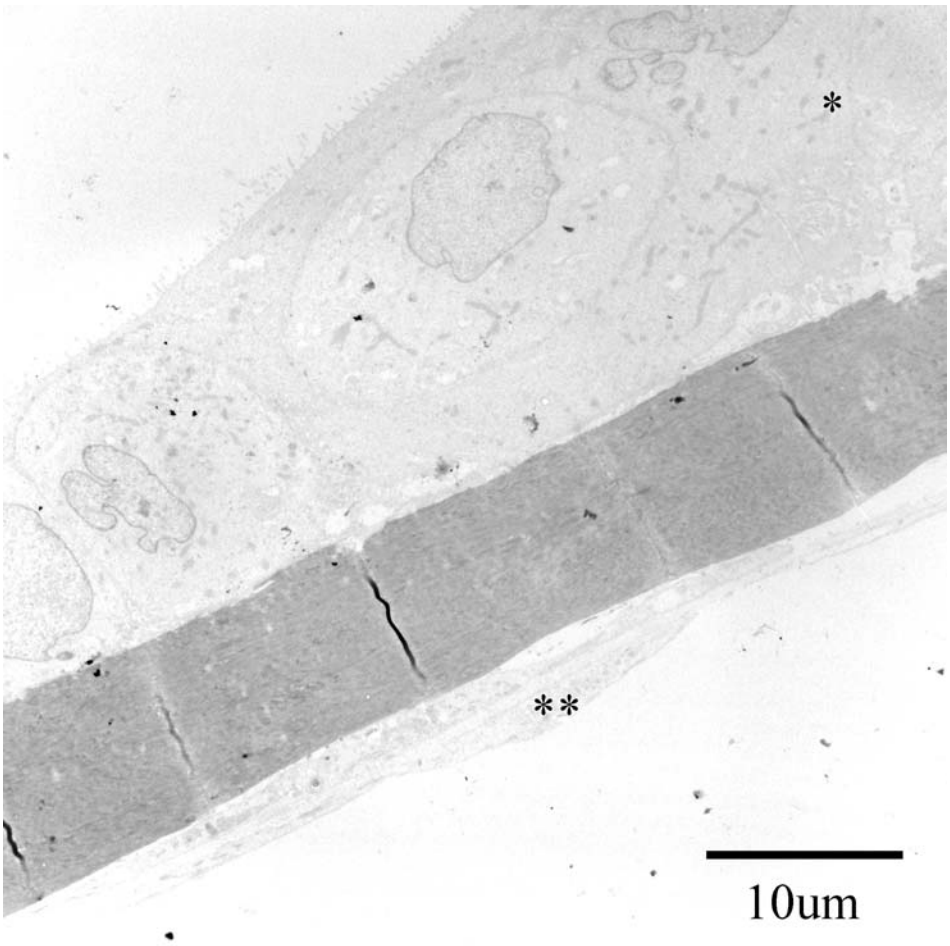

Figure 5. Thin collagen film serves as respiratory membrane in co-culture with pneumocytes (*) on top and endothelial cells on bottom (**). The collagen film is 8.6 microns thick.

silicone membranes is more robust than the O_2 exchange. Our recent investigations have not found a clear impact of channel size on efficiency of CO_2 transfer but it does appear that smaller channel size may have more efficient CO_2 exchange as would be expected.

The minimum channel size would be able to be reduced considerably if the channels were endothelialized. Although a resorbable scaffold and a completely engineered tissue based lung is the eventual goal, there may be an intermediate design step that includes endothelialized channels with non-resorbable scaffold components that would allow the minimum vascular channel size to be reduced considerably.

The current engineered lung scaffolds are manufactured utilizing silicone with soft lithography techniques that are standard in microfluidics. This is an intermediary scaffold that is a step in the development process of creating a resorbable scaffold that is suitable for gas exchange and seeding with lung epithelial and endothelial cells. The silicone scaffold is not suitable for cellularization but may have clinical application as a lung assist device, possibly as a bridge to transplant for patients with end stage lung disease. Transitioning the scaffold to a resorbable material is an important next step. Traditional resorbable biomaterials may not be great candidates given the relative bulk that would be required to create the vascular and gas chambers of the scaffold. Collagen is currently being investigated as a possible scaffold material as it is very strong even in thin sheets and would be ideal for cell attachment. This would significantly decrease the size of the scaffold components and allow more efficient packing of the vascular and gas exchange chambers within the scaffold. Early work cellularizing collagen films for gas exchange has demonstrated good promise for this scaffold material. Shown in Figure 5 is a TEM cross-sectional image of a collagen film with an endothelial cell on one side and a pneumocyte (type II pneumocyte from cell line) demonstrating how this collagen film could be used as the fundamental architectural component to create an engineered lung (unpublished data). Preliminary data demonstrates that during *in vitro* culture for just two weeks with endothelial cells and pneumocytes, the thickness of the collagen membrane reduces, presumably by cellular remodeling. Ideally, these cells would generate the physiologic cues to remodel this collagen film to achieve something near the native respiratory membrane thickness

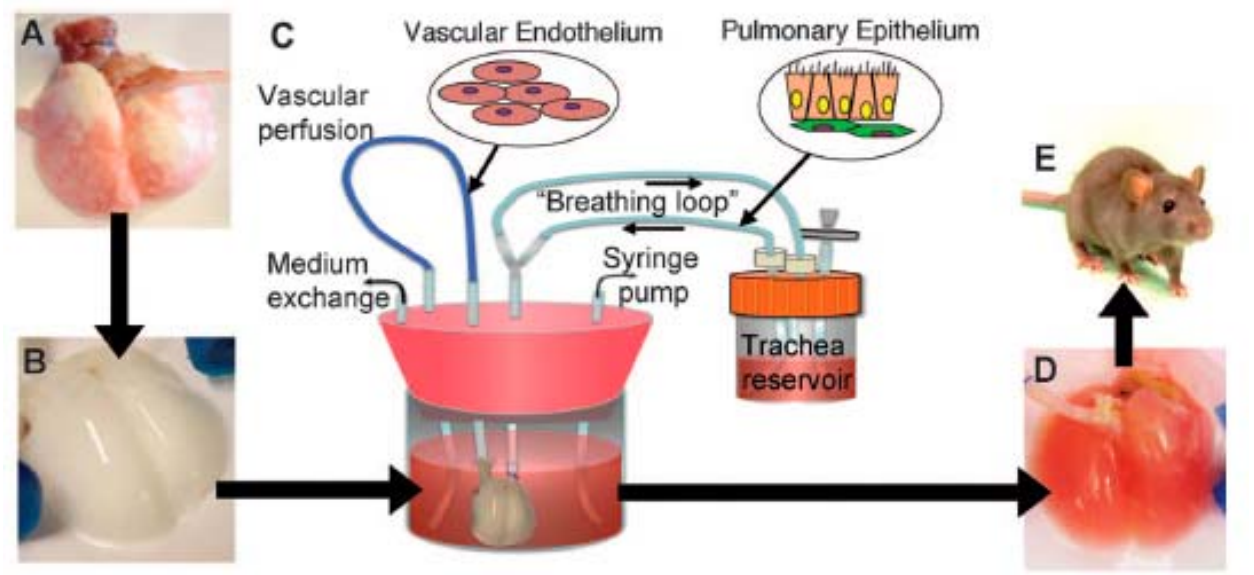

Figure 6. Scheme for lung tissue engineering. (A) Native adult rat lung is cannulated in the pulmonary artery and trachea for infusion of decellularization solutions. (B) Acellular lung matrix is devoid of cells after 2 to 3 hours of treatment. (C) Acellular matrix is mounted inside a biomimetic bioreactor that allows seeding of vascular endothelium into the pulmonary artery and pulmonary epithelium into the trachea. (D) After 4 to 8 days of culture, the engineered lung is removed from the bioreactor and is suitable for implantation into (E) the syngeneic rat recipient. Reproduced with permission from (16).

of an alveolus. Over time, it is expected that the original film would be completely replaced by cellular derived basement membrane components.

4. DECELLULARIZED APPROACH

Given the exquisite architecture of the native lung and the alveolar capillary interface, development of a elastic scaffold with sufficient surface area for gas transfer across a cellularized respiratory membrane is an enormous challenge. Following the recent progress in decellularization of solid organs including the heart and liver (31, 32) several groups have begun to develop decellularization and recellularization processes to create engineered lungs based upon native extracellular lung scaffolds. There have been early demonstrations of the feasibility of this approach in animal models.

The Niklason goup decellularized rat lungs using a perfusion solution containing 3- ((3-holamidopropyl)dimethylammonio)-1-propanesulfonate (CHAPS), a zwitterionic detergent (16). Their process generated an acellular lung matrix with preserved airway and vascular structures (Figure 6). They demonstrated retention of collagen as well as approximately 40% of the native elastin but under 10% of the native sulfated glycosaminoglycans (GAGs). These lung matrices were seeded with neonatal rat lung epithelial cells and microvascular long endothelial cells in a physiologic bioreactor. After one week of *ex vivo* growth, a left lung was implanted in the left chest in a rat model and perfused for 45 to 120 min. Gas exchange analysis demonstrated that the engineered lung is capable of fully saturating blood with oxygen up to pO_2 of 283 mmHg with sufficient removal carbon dioxide. The resulting engineered lung had microarchitecture very similar to native lungs with excellent cellularization throughout the scaffold.

Building on his pioneering work with decellularized hearts, Ott and co-workers also have developed methodologies to create engineered lungs using a decellularized matrix (15). For their decellularization technique, a sodium dodecyl sulfate (SDS)-based perfusion solution was used to generate cell free lungs with preserved alveolar and vascular structures. Using neonatal rat lung epithelial cells and human endothelial cells the matrices were recellularized with resulting architecture and alveolar number similar to native lungs. Implantation of a recellularized lung and the left chest resulted in a radiographically appearing normal lung that demonstrated oxygen exchange (Figure 7). These rats with one native lung one recellularized lung were able to be extubated and survived for several hours, breathing room air spontaneously before eventually succumbing to pulmonary edema.

Decellularization of mouse lungs has also been demonstrated using a Triton X-100 and sodium deoxycholate perfusion solution with DNase (33). These acellular lung matrices were mounted in a custom bioreactor capable of ventilating the lung scaffolds. These scaffolds demonstrated retained collagen similar to native lungs. Elastin content was only reduced to 63% of the native lung amounts and laminin and GAGs are also present in the decellularized extracellular matrix (ECM). Recellularization of the alveolar airway spaces with fetal mouse lung cells achieved growth of alveolar type II cells within the scaffold. Development of a decellularized mouse

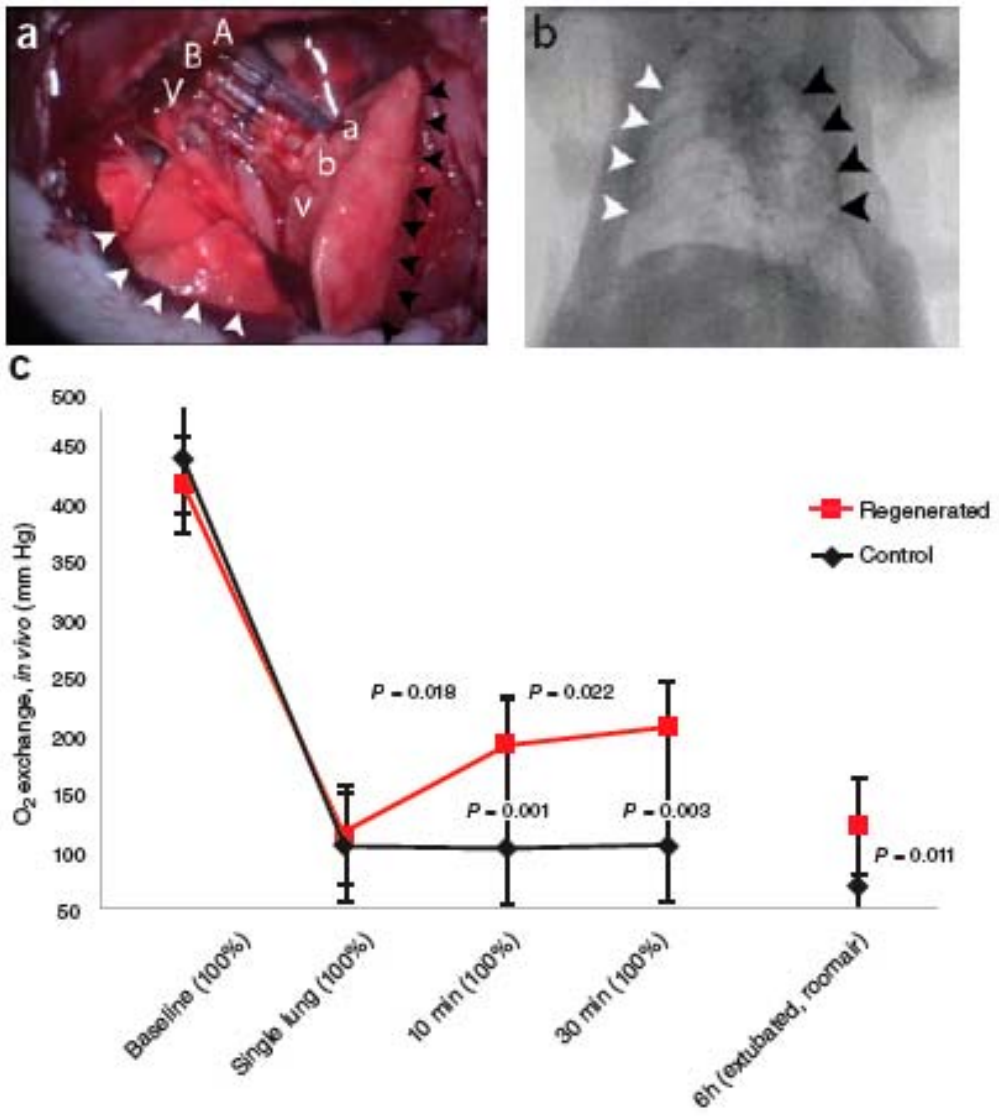

Figure 7. Orthotopic transplantation and *in vivo* function. (a) Photograph of left rat chest after left anterior thoracotomy, left pneumonectomy, and orthotopic transplantation of regenerated left lung construct. Recipient left pulmonary artery (A), left main bronchus (B), and left pulmonary vein (V) are connected to regenerated left lung pulmonary artery (a), bronchus (b), and pulmonary vein (v) White arrowheads, the recipient's right lung (infracardiac and right lower lobe); black arrowheads, the regenerated left lung construct. (b) Radiograph of rat chest after left pneumonectomy and orthotopic transplantation of a regenerated left lung construct. White arrowheads, recipient's right lung; black arrowheads regenerated left lung construct. (c) Results of blood gas analyses showing decrease in arterial oxygen tension (PaO_2) after left pneumonectomy and partial recovery after orthotopic transplantation of a regenerated left lung construct. Baseline, single lung, 10 min and 30 min measurements were obtained with the rat intubated and ventilated at volume control ventilation; 6 h measurements were obtained with the rat extubated and breathing room air without support of a ventilator. Upper P values compare single lung ventilation to 5 min, and 30 min time points after transplantation. Lower P values compare pneumonectomy to transplantation at 5 min, 30 min and 6 hour time points after operation. Error bars, s.d. Reproduced with permission from (15).

ung scaffold may prove to be very useful is able to be decellularized implanted in a mouse model. This has been accomplished with orthotopic mouse lung transplant (34). This would open the door for utilizing transgenic and knockout transplant host mice to elucidate the details of physiologic response to the maturation of these engineered lungs. The cell source for the lung epithelial and endothelial cells for these engineered lungs remains an outstanding question. Having molecular tools available for analysis of these transplanted organs and the host response to a variety of lung cells would be ideal.

Whole rat lung decellularization has also been demonstrated by continuous mechanical agitation in an

SDS solution following repeated lung freezing/thawing cycles (35). The resultant lung ECM was then utilized as a basement membrane for the culture of embryonic stem cells (ESC) to evaluate the effect of the ECM on driving these cells toward differentiation into lung cells. The lung ECM was compared to other potential ECM materials including Matrigel, Gelfoam and a type I collagen/pluronic F-127 hydrogel matrix. The ESCs had a higher retention and growth of seeded cells on the decellularized lung matrix compared to Matrigel, Gelfoam and collagen/pluronic matrix. The ESCs also had less apoptosis on the decellularized lung matrix compared to the other materials except Gelfoam which was similar. The ESCs also had more differentiation toward endothelial and epithelial cell types on the decellularized lung matrix as evidenced by higher staining levels of CD31, cytokeratin and pro-surfactant protein C (pro-SPC). Decellularized whole lungs were also reseeded with ESCs and demonstrated recellularization with evidence of differentiation with endothelial and epithelial markers observed including pro-SPC positive cells lining cyst like structures and the production of a measurable amount of surfactant protein A. ESCs cultured on decellularized lung ECM and within a completely decellularized lung progress towards endothelial and lung epithelial differentiation more efficiently than ECSs grown on other matrix materials. This evidence is an important step in the process of determining the cells that may be used to repopulate these decellularized lung matrices. Certainly, iPS cells or would be an ideal autologous cell source if they could be efficiently differentiated toward lung lineages within a decellularized ECM

These reports highlight an exciting new methodology in engineering lung tissues. Niklason and Ott both demonstrated decellularization of human or human sized lung tissues as a step towards clinical application of this approach. As highlighted by these authors many hurdles still remain, including clinical source of airway, alveolar and endothelial cells. Optimization of the decellularization recellularization protocols certain to occur. Likewise, the preimplantation culture techniques and maturation of these lungs *ex vivo* will be improved.

5. AIRWAY TISSUE ENGINEERING

Common approaches used to engineer other tissues have also been applied engineering airways. The approaches can be categorized by the following methods used to recreate the structures: "scaffold-free," naturally derived materials, synthetic materials, and combinations of the three (36). The "scaffold free" methods utilize cell sheets and aggregate techniques to assemble the desired architectures. Unfortunately, this method typically suffers from a lack of sufficient mechanical strength to provide structure, particularly in applications like a trachea. Naturally derived materials typically used include collagen, fibrin, and hyaluronic-acid. When tissues are decellularized, detergents are used to wash away all cells while leaving the extracellular matrix intact. This remaining matrix is comprised of collagen proteins and has been shown to be an excellent scaffold material. Frequently used are synthetics materials include polyglycolic acid (PGA), polylactic acid (PLA), poly (lactic-co-glycolic acid) (PLGA), silicone, and polytetrafluoroethelyene (PTFE). All of those materials, except PTFE and silicone, have adjustable degradation rates and are relatively easy to process.

Although the tissue engineering community has been slow to get products into the clinic, work in Europe has pushed engineered airways into experimental human use using naturally derived materials. The first documented case use of a tissue engineered airway was performed by Macchiarini *et al* in 2003 (37). In this case, a porcine jejunum segment was harvested and decellularized. Muscle cells and fibroblasts were isolated from a biopsy from the recipient. These cells were seeded on the decellularized collagen matrix and cultured in a bioreactor for several weeks to allow for integration with the scaffold. The structure was then folded over to double the graft thickness, and implanted.

In 2008, Macchiarini *et al.* performed a similar reconstruction, but this time with a cadaveric trachea to replace the left main bronchus of a 30-year-old woman (38). For this case, the donor trachea was decellularized and then donor epithelial cells and mesenchymal stem-cell-derived chondrocytes were added to the scaffold. The cells and construct were cultured in a custom bioreactor for four days and then implanted into the recipient.

By 2010, at least three more airway reconstructions had been performed. Two of the three (including one 10-year-old boy) utilized decellularized cadaveric tracheas were seeded with the recipients own stem cells, and immediately implanted (39). The third case took a cadaveric trachea that was initially transplanted it in the forearm of the recipient (40). The recipient received immunosuppressive therapy that was slowly decreased over four months until it was stopped completely. Following the completion of immunosuppressive therapy, the trachea was transferred from the arm to replace the host trachea.

An important potential limitation of utilizing decellularized human trachea as a scaffold is availability of these constructs and in particular in sizes to match the intended recipient. To overcome this limitation, the Macchiarini group developed a trachea scaffold using polyurethane based biomaterials. The first clinical application of this technology utilized a scaffold custom built to the dimensions of the recipient (41). The scaffold was seeded with autologous bone marrow mononuclear cells in culture in the bioreactor for 36 hours prior to implantation. Immediately before transplantation, the scaffold was seeded a second time with autologous bone marrow mononuclear cells. The replaced airway included the distal 6 cm of the trachea, the right mainstem bronchus and 2 cm of the left mainstem bronchus. At four months, the patient had improved pulmonary function tests compared to preoperative testing. Bronchoscopy revealed a healthy epithelium with evidence of partial lining with a respiratory mucosa.

Most of these human cases are still relatively recent, and long term results from both human and large

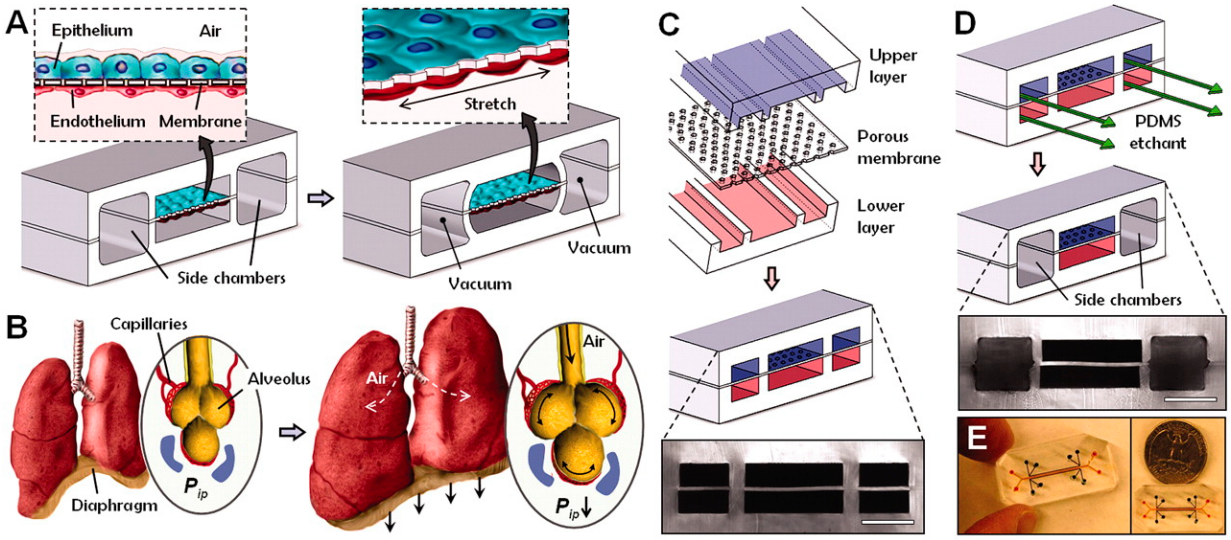

Figure 8. Biologically inspired design of a human breathing lung-on-a-chip microdevice. (A) The microfabricated lung mimic device uses compartmentalized PDMS microchannels to form an alveolar-capillary barrier on a thin, porous, flexible PDMS membrane coated with ECM. The device recreates physiologic breathing movements by applying vacuum to the side chambers and causing mechanical stretching of the PDMS membrane forming the alveolar-capillary barrier. (B) During inhalation in the living lung, contraction of the diaphragm causes a reduction in intrapleural pressure (P_{ip}), leading to distension of the alveoli and physical stretching of the alveolar-capillary interface. (C) Three PDMS layers are aligned and irreversibly bonded to form two sets of three parallel microchannels separated by a 10-microns-thick PDMS membrane containing an array of through holes with an effective diameter of 10 microns. Scale bar, 200 microns. (D) After permanent bonding, PDMS etchant is flowed through the side channels. Selective etching of the membrane layers in these channels produces two large side chambers to which vacuum is applied to cause mechanical stretching. Scale bar, 200 microns. (E) Images of actual lung-on-a-chip microfluidic device viewed from above. Reproduced with permission from (17).

animal studies are necessary in order to better understand the strengths and weaknesses of the various methods and conditions. Progress from the stem cell community will also provide assistance in selecting ideal cell types and determining whether *in vitro* culture is necessary. Although only relatively few cases of human tissue engineered airway reconstructions have been reported, more will surely follow.

6. TISSUE ENGINEERED LUNG AS *IN VITRO* MODEL

With the advent of the field of microfluidics and soft lithography (42), researchers have been working to develop *in vitro* test systems, and the lung is no exception. With time, these *in vitro* systems are getting increasingly complex. Initial microfluidic model lung devices featured a air liquid interface model with flowing fluid on the endothelial cell side (43). A recent device incorporated controlled air and blood flow as well as strain to the model respiratory membrane (17). This particular system was comprised of two channels (one for blood and the other for air) separated by a 10 um thick porous PDMS membrane, and was created in such a way that the membrane could be stretched to achieve physiologic strain levels and rates (Figure 8). In this anatomical analog of the natural alveolus, lung epithelial cells were grown on the air side of the membrane and endothelial cells grown on the blood side. Studies demonstrated that strain played a key role in nanoparticle transport through the membrane. This strain modeling membrane also was used to study the migration of neutrophils from the endothelial surface to the epithelial surface to engulf bacteria. These devices will continue to evolve and will be efficient in modeling particular controlled aspects of the alveolar barrier.

7. FUTURE PERSPECTIVES

Clinical based therapies of lung assist devices or engineered lung tissues are still several years away, yet recent progress with these technologies highlight the potential advantages of these approaches. Design optimization and scaling to a clinical sized device are the principle next steps of the microfluidic based lung assist device technology. It is first targeted as an acellular device for adult use with anticoagulation but eventually conversion to a biomimetic scaffold with endothelial cells will make it applicable as a pediatric and even neonatal device with reduced anticoagulation requirements. Refinement of decellularized scaffolds and seeding approaches are the focus of creating fully functional lungs for transplant. The key barriers are the particular cell source and the maturation of these constructs *in vitro* and *in vivo* to reach a stable point of cell turnover and function without degradation of the architecture. Initial small animal implants will progress to large animal decellularized constructs and implants to further assess the applicability of this approach for clinical therapy. Very encouraging results of decellularized trachea constructs being successfully implanted suggest that the solid organs

developed in a similar manner are distinctly possible. Finally, *in vitro* models of lung function and disease have been developed and will emerge as systems to study lung pathology.

8. ACKNOWLEDGEMENTS

The authors gratefully acknowledge support from the NIH (F32 DK076349-01, DMH).

9. REFERENCES

1. Dagalakis N, Flink J, Stasikelis P, Burke JF, Yannas IV. Design of an artificial skin. Part III. Control of pore structure. J *Biomed Mater Res* 14, 511-528 (1908)

2. Yannas IV, Burke JF, Gordon PL, Huang C, Rubenstein RH. Design of an artificial skin. II. Control of chemical composition. *J Biomed Mater Res* 14, 107-132 (1980)

3. Yannas IV, Burke JF. Design of an artificial skin. I. Basic design principles. *J Biomed Mater Res* 14, 65-81 (1980)

4. Ehrenreich M, Ruszczak Z. Update on tissue-engineered biological dressings. *Tissue Eng* 12, 2407-2424 (2006)

5. L'Heureux N, Dusserre N, Konig G, Victor B, Keire P, Wight TN, *et al.* Human tissue-engineered blood vessels for adult arterial revascularization. *Nat Med* 12, 361-365 (2006)

6. McAllister TN, Maruszewski M, Garrido SA, Wystrychowski W, Dusserre N, Marini A, *et al.* Effectiveness of haemodialysis access with an autologous tissue-engineered vascular graft: a multicentre cohort study. *Lancet* 373, 1440-1446 (2009)

7. Jayo MJ, Jain D, Ludlow JW, Payne R, Wagner BJ, McLorie G, *et al.* Long-term durability, tissue regeneration and neo-organ growth during skeletal maturation with a neo-bladder augmentation construct. *Regen Med* 3, 671-682 (2009)

8. Haider H, Lei Y, Ashraf M. MyoCell, a cell-based, autologous skeletal myoblast therapy for the treatment of cardiovascular diseases. *Curr Opin Mol Ther* 210, 611-621 (2010)

9. Camboni D, Philipp A, Arlt M, Pfeiffer M, Hilker M, Schmid C. First experience with a paracorporeal artificial lung in humans. *ASAIO J* 55, 304-306 (2009)

10. Ricci D, Boffini M, Del Sorbo L, El Qarra S, Comoglio C, Ribezzo M, *et al.* The use of CO2 removal devices in patients awaiting lung transplantation: an initial experience. *Transplant Proc* 42, 1255-1258 (2010)

11. Bartosik W, Egan JJ, Wood AE. The Novalung interventional lung assist as bridge to lung transplantation for self-ventilating patients - initial experience. *Interact Cardiovasc Thorac Surg* 13, 198-200 (2011)

12. Lee JK, Kung HH, Mockros LF. Microchannel technologies for artificial lungs: (1) theory. *ASAIO* J 54, 372-382 (2008)

13. Burgess KA, Hu HH, Wagner WR, Federspiel WJ. Towards microfabricated biohybrid artificial lung modules for chronic respiratory support. *Biomed Microdevices* 11, 117-127 (2009)

14. Hoganson DM, Anderson JL, Weinberg EF, Swart EJ, Orrick BK, Borenstein JT, *et al.* Branched vascular network architecture: a new approach to lung assist device technology. *J Thorac Cardiovasc Surg* 140, 990-995 (2010)

15. Ott HC, Clippinger B, Conrad C, Schuetz C, Pomerantseva I, Ikonomou L, *et al.* Regeneration and orthotopic transplantation of a bioartificial lung. *Nat Med* 16, 927-933 (2010)

16. Petersen TH, Calle EA, Zhao L, Lee EJ, Gui L, Raredon MB, *et al.* Tissue-engineered lungs for *in vivo* implantation. *Science* 329, 538-541 (2010)

17. Huh D, Matthews BD, Mammoto A, Montoya-Zavala M, Hsin HY, Ingber DE. Reconstituting organ-level lung functions on a chip. *Science* 328, 1662-1668 (2010)

18. Koike N, Fukumura D, Gralla O, Au P, Schechner JS, Jain RK. Tissue engineering: creation of long-lasting blood vessels. *Nature* 428, 138-139 (2004)

19. Levenberg S, Rouwkema J, Macdonald M, Garfein ES, Kohane DS, Darland DC, *et al.* Engineering vascularized skeletal muscle tissue. *Nat Biotechnol* 23, 879-884 (2005)

20. Au P, Tam J, Fukumura D, Jain RK. Bone marrow-derived mesenchymal stem cells facilitate engineering of long-lasting functional vasculature. *Blood* 111, 4551-4558 (2008)

21. Griffith LG, Wu B, Cima MJ, Powers MJ, Chaignaud B, Vacanti JP. *In vitro* organogenesis of liver tissue. *Ann N Y Acad Sci* 831, 382-397 (1997)

22. Kaihara S, Borenstein J, Koka R, Lalan S, Ochoa ER, Ravens M, *et al.* Silicon micromachining to tissue engineer branched vascular channels for liver fabrication. *Tissue Eng* 6, 105-117 (2006)

23. Hoganson DM, Pryor HI, 2nd, Spool ID, Burns OH, Gilmore JR, Vacanti JP. Principles of biomimetic vascular network design applied to a tissue-engineered liver scaffold. *Tissue Eng Part A*; 16, 1469-1477 (2010)

24. Hoganson DM, Pryor HI, 2nd, Bassett EK, Spool ID, Vacanti JP. Lung assist device technology with physiologic blood flow developed on a tissue engineered scaffold platform. *Lab Chip* 11, 700-707 (2010)

25. Malek AM, Alper SL, Izumo S. Hemodynamic shear stress and its role in atherosclerosis. *Jama* 282, 2035-2042 (1999)

26. Page TC, Light WR, Hellums JD. Prediction of microcirculatory oxygen transport by erythrocyte/hemoglobin solution mixtures. *Microvasc Res* 56, 113-126 (1998)

27. Page TC, Light WR, Hellums JD. Oxygen transport in 10 microns artificial capillaries. *Adv Exp Med Biol* 471, 715-721 (1999)

28. Page TC, Light WR, McKay CB, Hellums JD. Oxygen transport by erythrocyte/hemoglobin solution mixtures in an *in vitro* capillary as a model of hemoglobin-based oxygen carrier performance. *Microvasc Res* 55, 54-64 (1998)

29. Kung MC, Lee JK, Kung HH, Mockros LF. Microchannel technologies for artificial lungs: (2) screen-filled wide rectangular channels. *ASAIO J* 54, 383-389 (2008)

30. Lee JK, Kung MC, Kung HH, Mockros LF. Microchannel technologies for artificial lungs: (3) open rectangular channels. *ASAIO J* 54, 390-395 (2008)

31. Ott HC, Matthiesen TS, Goh SK, Black LD, Kren SM, Netoff TI, *et al.* Perfusion-decellularized matrix: using nature's platform to engineer a bioartificial heart. *Nat Med* 14, 213-221 (2008)

32. Uygun BE, Soto-Gutierrez A, Yagi H, Izamis ML, Guzzardi MA, Shulman C, *et al.* Organ reengineering through development of a transplantable recellularized liver graft using decellularized liver matrix. *Nat Med* 16, 814-820 (2010)

33. Price AP, England KA, Matson AM, Blazar BR, Panoskaltsis-Mortari A. Development of a decellularized lung bioreactor system for bioengineering the lung: the matrix reloaded. *Tissue Eng Part A* 16, 2581-2591 (2011)

34. Okazaki M, Krupnick AS, Kornfeld CG, Lai JM, Ritter JH, Richardson SB, *et al.* A mouse model of orthotopic vascularized aerated lung transplantation. *Am J Transplant* 7, 1672-1679 (2007)

35. Cortiella J, Niles J, Cantu A, Brettler A, Pham A, Vargas G, *et al.* Influence of acellular natural lung matrix on murine embryonic stem cell differentiation and tissue formation. *Tissue Eng Part A* 16, 2565-2580 (2010)

36. Ott LM, Weatherly RA, Detamore MS. Overview of tracheal tissue engineering: clinical need drives the laboratory approach. *Ann Biomed Eng* 39, 2091-2113 (2011)

37. Macchiarini P, Walles T, Biancosino C, Mertsching H. First human transplantation of a bioengineered airway tissue. *J Thorac Cardiovasc Surg* 128, 638-641 (2004)

38. Macchiarini P, Jungebluth P, Go T, Asnaghi MA, Rees LE, Cogan TA, *et al.* Clinical transplantation of a tissue-engineered airway. *Lancet* 372, 2023-2030 (2008)

39. Laurance J. British boy receives trachea transplant built with his own stem cells. *BMJ* 340, c1633 (2010)

40. Delaere P, Vranckx J, Verleden G, De Leyn P, Van Raemdonck D. Tracheal allotransplantation after withdrawal of immunosuppressive therapy. *N Engl J Med* 362, 138-145 (2010)

41. Jungebluth P, Alici E, Baiguera S, Le Blanc K, Blomberg P, Bozoky B, *et al.* Tracheobronchial transplantation with a stem-cell-seeded bioartificial nanocomposite: a proof-of-concept study. *Lancet* 378, 1997-2004 (2011)

42. Whitesides GM, Ostuni E, Takayama S, Jiang X, Ingber DE. Soft lithography in biology and biochemistry. *Annu Rev Biomed Eng* 3, 335-373 (2001)

43. Nalayanda DD, Wang Q, Fulton WB, Wang TH, Abdullah F. Engineering an artificial alveolar-capillary membrane: a novel continuously perfused model within microchannels. *J Pediatr Surg* 45, 45-51 (2010)

Abbreviations: iPS – Induced Pluripotent Stem Cell, PDMS – Polydimethylsiloxane, Review

Key Words: Tissue Engineering, Scaffold, Decellularize, Biomimetic, Vascular Network, Trachea, Review

Send correspondence to: Joseph P. Vacanti, Department of Pediatric Surgery, 55 Fruit Street, Warren 1151, Boston, MA 02114 Tel: 617-724-1725; Fax: 617-726-2167, E-mail: jvacanti@partners.org